

# Recovery of Encapsulated Adult Neural Progenitor Cells from Microfluidic-Spun Hydrogel Fibers Enhances Proliferation and Neuronal Differentiation

Bhavika B. Patel, Marilyn C. McNamara, Laura S. Pesquera-Colom, Emily M. Kozik, Jasmin Okuzonu, Nicole N. Hashemi, and Donald S. Sakaguchi\*



Cite This: *ACS Omega* 2020, 5, 7910–7918



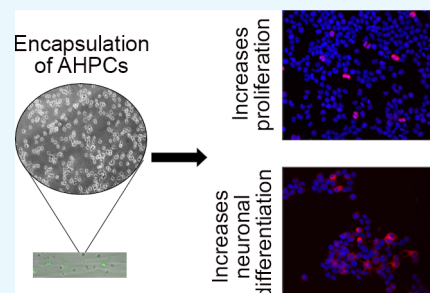
Read Online

ACCESS |

Metrics & More

Article Recommendations

**ABSTRACT:** Because of the limitations imposed by traditional two-dimensional (2D) cultures, biomaterials have become a major focus in neural and tissue engineering to study cell behavior *in vitro*. 2D systems fail to account for interactions between cells and the surrounding environment; these cell–matrix interactions are important to guide cell differentiation and influence cell behavior such as adhesion and migration. Biomaterials provide a unique approach to help mimic the native microenvironment *in vivo*. In this study, a novel microfluidic technique is used to encapsulate adult rat hippocampal stem/progenitor cells (AHPCs) within alginate-based fibrous hydrogels. To our knowledge, this is the first study to encapsulate AHPCs within a fibrous hydrogel. Alginate-based hydrogels were cultured for 4 days *in vitro* and recovered to investigate the effects of a 3D environment on the stem cell fate. Post recovery, cells were cultured for an additional 24 or 72 h *in vitro* before fixing cells to determine if proliferation and neuronal differentiation were impacted after encapsulation. The results indicate that the 3D environment created within a hydrogel is one factor promoting AHPC proliferation and neuronal differentiation (19.1 and 13.5%, respectively); however, this effect is acute. By 72 h post recovery, cells had similar levels of proliferation and neuronal differentiation (10.3 and 8.3%, respectively) compared to the control conditions. Fibrous hydrogels may better mimic the natural micro-environment present *in vivo* and be used to encapsulate AHPCs, enhancing cell proliferation and selective differentiation. Understanding cell behavior within 3D scaffolds may lead to the development of directed therapies for central nervous system repair and rescue.



## INTRODUCTION

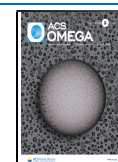
Neurodegenerative diseases and injury can lead to severe deficits in the sensory, motor, and cognitive function, prompting researchers to investigate and develop novel therapeutic strategies targeting these conditions. Cellular therapies, including stem and progenitor cell transplants, may be used as a means for aiding regeneration by (1) directing those cells to differentiate into specific neurons or glial cells for cell replacement or (2) to serve as a source of neurotrophic/growth factors to enhance neuroprotection and repair. Multipotent adult neural stem/progenitor cells (NSCs) are an appealing source of cells to study and use in transplantation because of their ability to differentiate into neurons, astrocytes, and oligodendrocytes.<sup>1</sup> Furthermore, it is important to study these cells in a more native environment, rather than in a two-dimensional (2D) system. Traditional 2D cultures fail to reliably mimic the natural microenvironment present within the tissues.<sup>2</sup> Therefore, recent advances in tissue engineering have largely focused on using biomaterials in combination with cells as a means to better understand their three-dimensional (3D) microenvironment present *in vivo*.

Encapsulating cells during scaffold formation provides a structural support similar to that of the tissue microenvironment.<sup>3</sup> Scaffolds such as hydrogels are ideal for cell encapsulation because they provide a 3D framework in which the mechanical properties can be tailored to specific tissue constructs. Hydrogels are cross-linked networks of polymers that swell when hydrated, providing an environment that mimics a more native tissue structure ideal for cell growth.<sup>4</sup> Polymerization processes employing natural and synthetic hydrogels have been used to encapsulate cells.<sup>5</sup> One such natural polymer is alginate, a Food and Drug Administration (FDA)-approved and biocompatible polymer that is found in brown algae and some bacteria.<sup>6,7</sup> Alginate can be gelled by ionic cross-linking, a cell-safe method which

Received: December 9, 2019

Accepted: March 20, 2020

Published: April 2, 2020



utilizes divalent cations to form ionic bridges, thus yielding a 3D network of a characteristic “egg-box” organization.<sup>8,9</sup> The rapid ionic interaction allows for high-speed gelation, thus allowing for more controllable and tunable mechanical and degradation properties.<sup>10–12</sup> Because of its tissue-like mechanical properties, it has been used in multiple areas of regenerative medicine including cartilage and bone repair, making it a versatile polymer for investigating tissue engineering<sup>13,14</sup> but also shows promise in neural applications. NSCs encapsulated within alginate beads proliferate and retain their metabolic functions, and recovered cells retain their ability to differentiate.<sup>15,16</sup> Additionally, because alginate is FDA-approved, several pharmaceutical products use it as a base for drug delivery<sup>17</sup> and wound dressing.<sup>18</sup>

To facilitate cell survival, cell encapsulation methods must be biocompatible and minimize the use of harsh conditions for polymerization. One approach is using a microfluidic platform, which is well-suited for a number of biomedical applications as well as gelation or polymerization *via* cross-linking of a core and sheath fluid.<sup>11,19–22</sup> Previous studies have used microfluidics to encapsulate cells within microparticles, microspheres, and microgels.<sup>23–26</sup> In addition to these applications, the microfluidic technique is capable of forming continuous fibers. The ability to adjust parameters such as concentrations of sheath and core fluids as well as flow rates provides more flexibility during the fabrication<sup>27</sup> and encapsulation process; however, it is important to match the viscosities of the core and sheath solution to minimize shear force at the fluid/fluid interface.<sup>28</sup> Furthermore, optimization is needed to ensure that the concentration of  $\text{CaCl}_2 \cdot 2\text{H}_2\text{O}$  within the sheath fluid was high enough to fully solidify the microfiber within the microfluidic device but not too high as to cause clogging within the channel. Flow rate ratios (FRRs) must also be optimized; if the fluids flow too quickly through the microfluidic device, time within the device will be insufficient to fully solidify the fiber, which will then solidify on contact with the coagulation bath, as in the extrusion method of fiber fabrication.<sup>11</sup> Similarly, flow rates that are too slow will cause clogging within the channel.

Because microfluidic fiber fabrication is cell-safe, it is possible to incorporate cells within the fiber construct either before or after fabrication.<sup>12,29</sup> Fibers are ideal for aiding in cell alignment and elongation during regeneration.<sup>30</sup> Aligned fibrous scaffolds also influence cellular morphological changes for cells, thus making them a platform for cell differentiation.<sup>31,32</sup> Furthermore, the native extracellular matrix (ECM) is a complex network that provides a physical structure for cell–cell interactions during tissue formation and maintenance.<sup>33</sup> In order to mimic the ECM *in vitro*, studies have utilized fibrous scaffolds to aid in cell–cell interactions and cell differentiation.<sup>2,34,35</sup> Although unmodified alginate hydrogels do not contain the necessary ligands and active sites to support cell–substrate interactions, their biocompatibility and favorable mechanical properties have made them a popular choice for 3D cell culturing.<sup>12,16,25,36–39</sup> However, inclusion of ECM agents such as collagen or peptides such as arginine–glycine–aspartic acid (RGD) can help cell adhesion and proliferation.<sup>7,40</sup> Furthermore, mesenchymal stem cells,<sup>41,42</sup> pluripotent stem cells,<sup>15,43</sup> and embryonic stem cells<sup>44</sup> have been encapsulated within the alginate, showing the broad uses of alginate in biomedical applications, and the present study consists of two major goals: the first aim is to utilize a microfluidic technique to encapsulate adult hippocampal

progenitor cells (AHPCs) within alginate hydrogels. Fibrous scaffolds are an area of interest in tissue engineering and regenerative medicine because they can mimic the native ECM, an important regulator of cell migration, cell fate determination, and dynamic behavior such as adhesion and proliferation.<sup>45,46</sup> Furthermore, fibrous scaffoldings can provide support for cell growth in specific geometries, providing control over their orientations and locations.<sup>35</sup> Second, to better understand the effects of the 3D environment created using the hydrogels, cells were recovered after encapsulation using a phosphate buffered saline (PBS) to investigate changes in proliferation and differentiation of the AHPCs post encapsulation. It is important to ensure that viable cells can be recovered, therefore cells were evaluated post encapsulation.

Here, we report the ability to encapsulate AHPCs within microfluidic-spun fibrous scaffolds. In a previous study, astrocytes have been encapsulated within alginate hydrogels using the same technique with similar parameters, and a live/dead assay showed that 89% of cells survived 24 h post encapsulation. This study also provided a detailed examination of the mechanical and physical properties of the microfibers.<sup>12</sup> The current study focuses on the use of neural stem cells and the impact hydrogels may have on cell biology. The encapsulation procedures impacted proliferation and neuronal differentiation of cells. Cell-encapsulated microfibers were cultured for 4 days *in vitro* ((DIV) although may be cultured for longer periods of time) prior to recovery in order to provide sufficient time to grow and proliferate within a 3D hydrogel. Our results demonstrate that recovered AHPCs had increased proliferation and neuronal differentiation after 24 h of recovery; however, by 72 h post recovery, there was no significant difference in cell proliferation or neuronal differentiation compared with control cells. Encapsulation of AHPCs within microfluidic-spun hydrogels can be used to direct cell differentiation and improve upon current transplantation strategies for nervous system rescue and repair.

## ■ EXPERIMENTAL SECTION

### Preparation of Microfluidic Devices and Channels.

The microfluidic mold used for this study was created on a silicon wafer using soft photolithography, as previously described.<sup>12,20,47,48</sup> The microchannel has dimensions of  $130 \mu\text{m} \times 390 \mu\text{m}$  (height  $\times$  width), and the microfluidic device features four chevrons, each  $130 \mu\text{m} \times 100 \mu\text{m}$  (height  $\times$  width) and spaced  $200 \mu\text{m}$  apart, which help in hydrodynamically focusing the core fluid while ensuring that the sheath solution can fully surround and solidify it. The length of the coagulation chamber was 8 mm.

Briefly, to create the microfluidic device, polydimethylsiloxane (PDMS, Dow Corning Corporation, Midland, MI) was mixed in a 1:10 ratio of the elastomer curing agent to elastomer base and was poured onto the molds. After allowing time for degassing, the two-halves were hardened at  $80 \text{ }^\circ\text{C}$  for 25 min. Layers were added via plasma cleaning on medium strength for 20 s for added thickness. The two halves were prepared using the same plasma cleaning process and then were aligned visually using a dissecting microscope. Microfluidic channels were generated using PDMS (IDEX Health and Science polymer tubing, 1.02 mm ID  $\times$  2.16 mm OD, Dow Corning Silastic), and Devcon Home 1:1 Epoxy. Devices were sterilized using 70% ethanol and a minimum of 5 h of exposure to ultraviolet light within a biological fume hood.

Finally, devices were sterilized via autoclaving before beginning encapsulation.

**Preparation of Solutions.** The pre-gel solution was made by dissolving 6% (g/mL) alginate (alginic acid sodium salt, very low viscosity, Alfa Aesar, Haverhill, MA) in Corning Cellgro Sterile WFI-Quality water at room temperature overnight. Before use, pre-gel solutions were filter-sterilized using syringe filters under pressure in the following sequence: 3  $\mu\text{m}$  pore size, 0.45  $\mu\text{m}$  pore size, and sterile 0.22  $\mu\text{m}$  pore size. Half of the prepared solution was stored at room temperature, while the other half was placed in the freezer for storage and later use. For the sheath fluid, a 0.5%  $\text{CaCl}_2 \cdot 2\text{H}_2\text{O}$  5% (calcium chloride dihydrate, C79, Fisher Scientific, Hampton, NH), 5% PEG (poly(ethylene glycol),  $M_n = 20,000$ , Sigma-Aldrich, St. Louis, MO) solution was created within deionized water and sterile-filtered with a 0.22  $\mu\text{m}$  pore size syringe filter.

**Cell Culture.** AHPCs were generously gifted by Dr. F. Gage (Salk Institute for Biological Sciences, La Jolla, CA). The AHPCs were isolated from Fischer 344 rats and were infected with a retrovirus to induce the expression of green fluorescent protein (GFP).<sup>49</sup> Previous studies from our laboratory have characterized the progenitor state of the AHPCs at various time points.<sup>34,50</sup>

The AHPCs were cultured in poly-L-ornithine (POL; 10  $\mu\text{g}/\text{mL}$ ; Sigma-Aldrich, St. Louis, MO) and laminin (10  $\mu\text{g}/\text{mL}$ ; R&D Systems, Minneapolis, MN) coated T-75 tissue culture flasks in maintenance media (MM) composed of Dulbecco's modified Eagle's medium/Ham's F-12 (DMEM/F-12, 1:1; Omega Scientific, Tarzana, CA) supplemented with 2.5 mM L-glutamine (GlutaMAX; Thermo Fisher Scientific, Waltham, MA), N2 supplement (Gibco BRL, Gaithersburg, MD), and 20 ng/mL basic fibroblast growth factor (bFGF; Promega Corporation, Madison, WI). Cells were maintained at 37  $^\circ\text{C}$  in 5%  $\text{CO}_2/95\%$  humidified air atmosphere. Half of the volume of cultured media was replaced with fresh MM every two days. To collect cells for encapsulation, they were detached using 0.05% trypsin-EDTA (Gibco BRL). Cell suspensions were collected and centrifuged at 280 rcf for 5 min and then resuspended in fresh MM.

**Cell Encapsulation.** The 6% alginate solutions were mixed in a 1:3 ratio with cell suspension (average of 7500 cells/ $\mu\text{L}$ ) within MM. The resulting mixture was placed into a 1 mL BD syringe and introduced with a constant flow into the core channel of the microfluidic device. Similarly, the sheath solution was pumped into the two side channels to help guide and solidify the core solution. A FRR of 250:10 ( $\mu\text{L}/\text{min}:\mu\text{L}/\text{min}$ ) sheath/core rate was used to fabricate all fibers. Upon exiting the microfluidic device, fibers were introduced into a 5%  $\text{CaCl}_2 \cdot 2\text{H}_2\text{O}$  collection bath and to further solidify resulting fibers. Fibers were gathered around pipette tips and were rinsed in PBS before releasing them within MM; approximately, 50–100  $\text{mm}^3$  of fibers were placed within each well. Hydrogels were cultured for 4 days in MM at 37  $^\circ\text{C}$  in 5%  $\text{CO}_2/95\%$  humidified air atmosphere.

To compare cells growing within hydrogels, two control conditions were also established in parallel: (1) cells were collected prior to addition of the alginate solution and (2) cells were subjected to the same alginate solution used to fabricate all fibers but without the polymerization step. Cells from these controls were collected and cultured on glass coverslips coated with poly-L-ornithine (10  $\mu\text{g}/\text{mL}$ ) and purified mouse laminin (5  $\mu\text{g}/\text{mL}$ ) (POL) diluted in Earle's Balanced Salt Solution

((EBSS) Gibco BRL). Cells grown in hydrogels and control conditions were cultured for 4 DIV.

**Cell Recovery.** After 4 DIV, fibers were collected from wells and centrifuged at 280 rcf for 5 min. The supernatant was discarded and the pellet was resuspended with 5 mL of sterile-filtered 0.1 M  $\text{PO}_4$  buffer (pH 7) for 20 min to depolymerize hydrogels. After 20 min, the fibers within the phosphate buffer were slowly triturated with a P100 pipette to help break down and dissociate the alginate microfibers and release cells. To further dissociate cells from alginate fibers, a P200 was used as well. The solution was centrifuged at 280 rcf for 5 min. The supernatant was discarded and the pellet was resuspended with fresh MM. The cells cultured under the control conditions were collected from the POL coverslips using 0.05% trypsin-EDTA in order to detach cells. After the cells detached, the cells were collected and placed in a conical tube with 5 mL of sterile-filtered 0.1 M  $\text{PO}_4$  buffer for 20 min, the same conditions as the cells encapsulated within the alginate fibers. Cells were centrifuged at 280 rcf for 5 min and the supernatant removed and the pellet resuspended in fresh MM. A Trypan blue (Gibco BRL) viable cell count was performed on the cell samples collected from the hydrogels and the two control conditions and the cells seeded onto POL-coated glass coverslips (12,000 cells/coverslip) from each condition. Cells from all conditions (recovered encapsulated cells, cells exposed to alginate solution and cells grown in MM) were collected using the same trituration and the 20 min incubation in 0.1  $\text{PO}_4$  buffer. This was done in order to account for any differences that may have been caused by mechanical manipulation during the collection. All cells were cultured at 37  $^\circ\text{C}$  in 5%  $\text{CO}_2/95\%$  humidified air atmosphere for either 24 or 72 h after recovery.

**Immunocytochemistry.** After 24 or 72 h after recovery, the cultured cells were rinsed twice with 0.1 M  $\text{PO}_4$  buffer, fixed with 4% paraformaldehyde (Fisher Scientific) in 0.1 M  $\text{PO}_4$  buffer for 20 min and then rinsed with PBS (Invitrogen, Carlsbad, CA) 3 times for 7 min each. Samples were incubated in blocking solution composed of 0.2% Triton X-100 (Thermo Fisher Scientific), 2.5% normal donkey serum (Jackson ImmunoResearch), 2.5% normal goat serum (Jackson ImmunoResearch), and 0.4% bovine serum albumin (Sigma-Aldrich) in PBS at room temperature for 1 h. Primary antibodies rabbit  $\alpha$  Ki-67 (16667, Abcam), mouse  $\alpha$  TuJ1 (MAB1195, R&D Systems), or mouse  $\alpha$  GFAP (MAB360, Millipore) were diluted in blocking solution and samples were incubated overnight at 4  $^\circ\text{C}$ . The next day, samples were rinsed 4 times for 8 min each with PBS and secondary antibodies (donkey anti-rabbit Cy3 or donkey anti-mouse Cy3 (1:500; Jackson ImmunoResearch) and 4',6-diamidino-2-phenylindole (DAPI) nuclear stain (1:50; Invitrogen) were diluted in blocking solution and incubated at room temperature for 90 min. After incubation, samples were rinsed four times for 8 min each in PBS. Samples were mounted onto glass slides using Vectashield with DAPI (Vector Laboratories; Burlingame, CA). Samples were stored at 4  $^\circ\text{C}$  in the dark until imaging.

**Imaging.** Immunocytochemistry samples were imaged using a Nikon Microphot FXA (Nikon Corp., Melville, NY, USA) microscope equipped with standard epifluorescence illumination and a Q imaging Retiga 2000R (Q Imaging, Burnaby, BC, Canada) digital camera. A 20 $\times$  objective was used to obtain images for quantitative data analysis. For the analysis, five microscopic fields were imaged per condition per sample, each field representing 0.24  $\text{mm}^2$ . A total of six



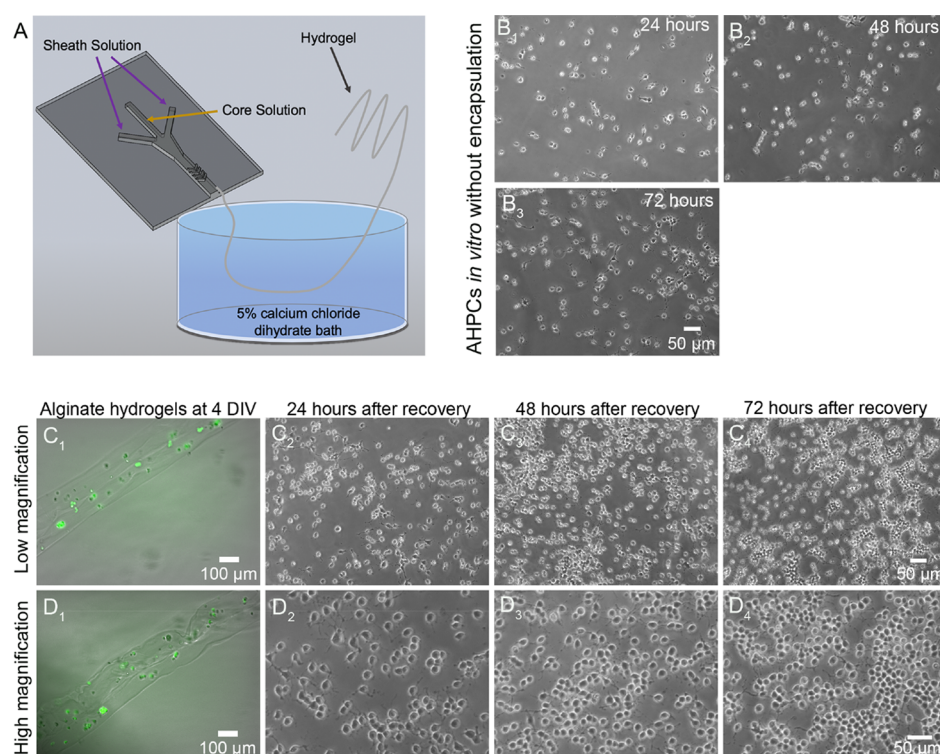


**Figure 1.** AHPCs encapsulated within fibrous hydrogels and recovered after 4 DIV. Proliferation of AHPCs post cell recovery *in vitro* indicate that cells survive following encapsulation within alginate hydrogels. (A) Schematic illustration of the microfluidic device. (B<sub>1</sub>–B<sub>3</sub>) AHPCs cultured in a standard 2D environment at 24, 48 and 72 h, respectively, *in vitro*. (C<sub>1</sub>,D<sub>1</sub>) GFP expressing AHPCs encapsulated within alginate hydrogels. (C<sub>2</sub>–C<sub>4</sub>) AHPCs recovered from hydrogels at 24, 48, and 72 h post recovery imaged using a 10x objective (top row). (D<sub>2</sub>–D<sub>4</sub>) AHPCs recovered from hydrogels at 24, 48, and 72 h post recovery imaged with 20× objective (bottom row). Scale bars = 50 μm.

independent experiments were conducted, with a total of 30 images quantified per antibody, per condition. A Zeiss LSM700 Confocal (Oberkochen, Germany) microscope equipped with an AxioCam MRC5 was used to image samples for high-resolution images with a 20× objective.

**Quantitative Data Analysis.** After immunocytochemical experiments and imaging, quantitative analysis was conducted using the Fiji software.<sup>51</sup> From each replicate, five imaging fields were chosen per sample for each primary antibody for a total of 30 imaging fields quantified. The following counts were made in each field to determine the percentage of immunolabeled cells for each respective antibody: total number of immunolabeled cells divided by the total number of cells (DAPI-stained nuclei). GraphPad Prism v6 software (GraphPad Software, Inc., La Jolla, CA, USA) was used for statistical analysis. An ordinary one-way ANOVA with multiple comparisons was used to compare the means across the conditions per antibody. A *p*-value of  $\leq 0.05$  was considered significant. Error bars represent the standard error of the mean.

## RESULTS

**Increase in Proliferation after Cell Recovery from Alginate Fibrous Hydrogels.** AHPCs were mixed in a 1:3 ratio with MM and introduced into a core channel of a microfluidic channel in order to encapsulate cells. Alginate fibers produced under similar conditions with an FRR of 125:10 ( $\mu\text{L}/\text{min}:\mu\text{L}/\text{min}$ ) had dry diameters of approximately 8 μm; therefore, fibers generated with an FRR of 250:10 ( $\mu\text{L}/\text{min}:\mu\text{L}/\text{min}$ ) will have smaller diameters because of the larger sheath fluid flow rate, which provides higher amounts of shear force on the core fluid.<sup>12</sup> Fibers fabricated within microfluidic

devices are continuously generated (Figure 1A) and therefore do not have a maximum length.<sup>35,52</sup> AHPCs cultured in 2D environments not exposed to the encapsulation process are shown in Figure 1B<sub>1</sub>–B<sub>3</sub>. Figure 1C<sub>1</sub>,D<sub>1</sub> shows phase contrast and fluorescent images at low and high magnifications of green fluorescent expressing (GFP)-AHPCs encapsulated within alginate hydrogels at 4 DIV. To assess changes in proliferation and differentiation, AHPCs were recovered from hydrogels using PBS which dissociates the hydrogel. Cells, including control condition cells, were collected and plated on POL-coated glass coverslips and cultured for an additional 24 or 72 h. After recovery, cells were monitored for normal growth *in vitro*, and it was evident that the cells continued to proliferate post recovery from 24 to 72 h and have short processes characteristic of the AHPCs *in vitro* (Figure 1C<sub>2</sub>–C<sub>4</sub>,D<sub>2</sub>–D<sub>4</sub>). These results demonstrate successful recovery of viable cells after encapsulation within alginate hydrogels.

To determine if encapsulation within alginate fibers affects AHPC proliferation, immunocytochemistry experiments were conducted after recovery to detect the Ki-67 antigen, a nuclear protein present during G1, S, G2, and M phases of the cell cycle.<sup>53</sup> Our results demonstrate that 24 h after cell recovery, significantly more AHPCs were proliferating compared to control conditions (Figure 2). Furthermore, when comparing the two control conditions, there were no significant differences demonstrating that the increase in proliferation of the recovered AHPCs may be attributed to the 3D environment provided by the hydrogels and not because of the alginate solution itself (Figure 2A<sub>1</sub>–A<sub>2</sub>,B<sub>1</sub>–B<sub>2</sub>,C<sub>1</sub>–C<sub>2</sub>). The percentage of Ki-67 immunolabeled AHPCs was  $6.1\% \pm 1.3$ ,  $11.9\% \pm 3.7$ , and  $19.1\% \pm 4.5$  (control cells in MM, alginate

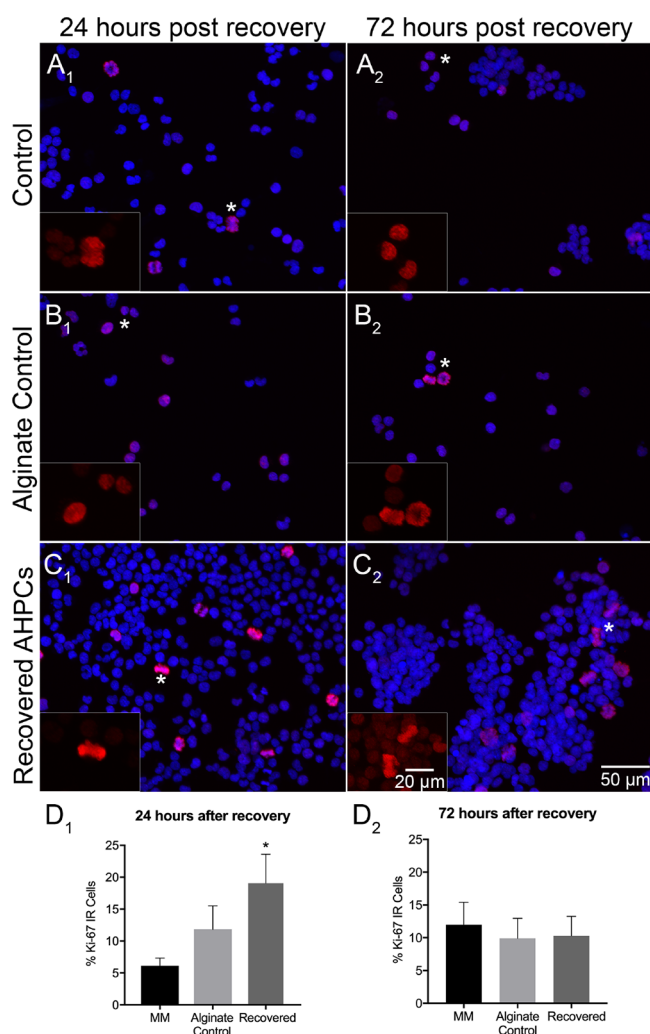


**Figure 2.** Proliferation of AHPCs following recovery after 4 days of encapsulation. Fluorescence images of AHPCs illustrating immunoreactivity for Ki-67 24 h after recovery (A<sub>1</sub>–C<sub>1</sub>) and 72 h after recovery (A<sub>2</sub>–C<sub>2</sub>): Ki-67-Cy3 (red) with DAPI staining (blue). AHPCs cultured in MM (A<sub>1</sub>,A<sub>2</sub>), alginate control (B<sub>1</sub>,B<sub>2</sub>), and recovered from hydrogels (C<sub>1</sub>,C<sub>2</sub>). Asterisks indicate the location of higher magnification inset images. Higher magnification images are of the Ki-67-Cy3 channel only. Scale bar = 50  $\mu$ m (20  $\mu$ m for insets). Abbreviations: DAPI, 4',6-diamidino-2-phenylindole. (D<sub>1</sub>,D<sub>2</sub>), Quantitative analysis of AHPCs immunoreactive for the Ki-67 antibody. Error bars represent the standard error of the mean.  $N = 6$  independent experiments, 5 imaging fields per experiment. \*Significantly different at  $p \leq 0.05$ .

solution control and recovered AHPCs), respectively (Figure 2D<sub>1</sub>,D<sub>2</sub>). When assessing proliferation after 72 h post recovery, no significant differences were found between all conditions. Taken together, these results may indicate that the increase in the number of AHPCs proliferating following recovery from the hydrogels may be due to the 3D fibrous environment of the hydrogel, not the alginate solution itself, and the alginate hydrogels may provide specific cues promoting cell proliferation.

**Recovered AHPCs Have Increased Neuronal Differentiation.** A number of studies have demonstrated that 3D scaffolds can be used to influence and direct cell differentiation without chemical inducers.<sup>34,35,38,54</sup> The multipotent AHPCs have the ability to differentiate into neurons, astrocytes, and

oligodendrocytes *in vitro*.<sup>55</sup> Neuronal differentiation of the AHPCs was characterized using the TuJ1 (class III  $\beta$ -tubulin) antibody, a marker for developing neurons.<sup>56,57</sup> Although some AHPCs in all conditions were immunopositive for TuJ1, there was an increase in TuJ1 immunoreactivity for cells after 24 h post recovery from the hydrogels (Figure 3A<sub>1</sub>–C<sub>1</sub>). The

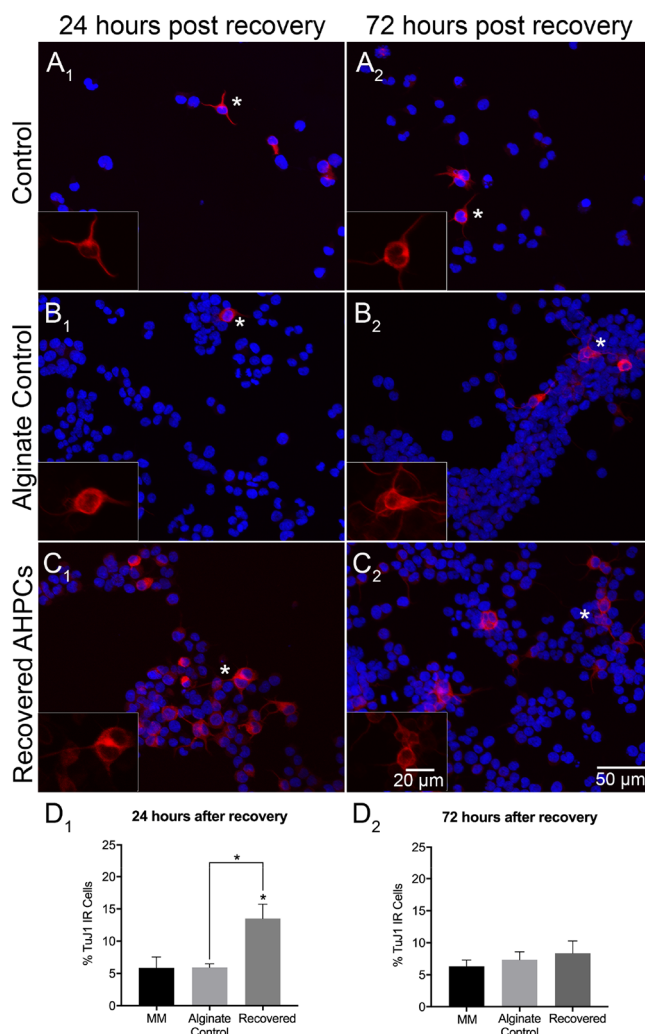


**Figure 3.** Neuronal differentiation of recovered AHPCs after 4 days of encapsulation. Fluorescence images of AHPCs illustrating immunoreactivity for TuJ1 24 h after recovery (A<sub>1</sub>–C<sub>1</sub>) and 72 h after recovery (A<sub>2</sub>–C<sub>2</sub>): TuJ1-Cy3 (red) with DAPI staining (blue). AHPCs cultured in MM (A<sub>1</sub>,A<sub>2</sub>), alginate control (B<sub>1</sub>,B<sub>2</sub>), and recovered from hydrogels (C<sub>1</sub>,C<sub>2</sub>). Asterisks indicate the location of higher magnification inset images. Higher magnification images are of the TuJ1-Cy3 channel only. Scale bar = 50  $\mu$ m (20  $\mu$ m for insets). Abbreviations: DAPI, 4',6-diamidino-2-phenylindole. (D<sub>1</sub>,D<sub>2</sub>), Quantitative analysis of AHPCs immunoreactive for the TuJ1 antibody. Error bars represent standard error of the mean.  $N = 6$  independent experiments, 5 imaging fields per experiment. \*Significantly different at  $p \leq 0.05$ .

percentage of TuJ1-immunolabeled AHPCs 24 h post recovery was  $5.9\% \pm 1.7$ ,  $5.9\% \pm 0.6$ , and  $13.5\% \pm 2.2$  compared to  $6.3\% \pm 1$ ,  $7.3\% \pm 1.2$ , and  $8.3\% \pm 1.9$  following 72 h post recovery (control cells in MM, alginate control and recovered AHPCs, respectively (Figure 3D<sub>1</sub>,D<sub>2</sub>). No significant differences were found after 72 h post recovery (Figure 3A<sub>2</sub>–C<sub>2</sub>). Results suggest that the 3D environment is providing unique



cues for cells to differentiate and this response is acute rather than long-term.

Lastly, to determine if alginate hydrogels affect glial differentiation of AHPCs, glial fibrillary acidic protein (GFAP) was used to determine if astrocytes were present after recovery (Figure 4A–C). While a small percentage of

Together, these results demonstrate that encapsulation of AHPCs within fibrous hydrogels influences proliferation and differentiation. A 3D environment created using the hydrogel influenced cell proliferation and differentiation *in vitro* and thus can be used to guide cell differentiation.

## DISCUSSION

Using the microfluidic technique, we have successfully encapsulated AHPCs within alginate-based fibrous hydrogels and cultured them for 4 DIV. Although no observable degradation occurred over the course of this experiment, alginate is known to degrade in physiological conditions.<sup>8</sup> Our results demonstrate that recovered AHPCs had an increase percentage of proliferating cells as well as immature neurons compared to cells cultured in control conditions, which may be attributed to the 3D environment provided by the hydrogels. Interestingly, this effect was short-term and only seen at 24 h; by 72 h, the percentage of cells positive for Ki-67 or TuJ1 was comparable to control conditions. Overall, our results demonstrate that the 3D environment enhanced AHPC proliferation and neuronal differentiation after encapsulation within hydrogels.

To encapsulate AHPCs within alginate-based fibrous hydrogels, a microfluidic platform was used because this technique is biocompatible compared to other techniques such as electrospinning, which requires high voltage and harsh methods to achieve polymerization.<sup>58</sup> To the best of our knowledge, there has been no report of successful encapsulation of AHPCs using the electrospinning method. However, there have been various reports of using the microfluidic technique for forming fibers.<sup>59–61</sup> Therefore, a microfluidic approach is ideal for cell encapsulation, which can lead to development of biomaterial-based therapeutic strategies.

Neural stem cells have previously been encapsulated within alginate-based hydrogels in order to study cell behavior *in vitro* and *in vivo*.<sup>62,63</sup> Banerjee and colleagues found that hydrogel modulus influences stem cell differentiation; particularly, hydrogels with elastic moduli similar to the brain tissue promoted encapsulated cells toward a neuronal lineage. However, this study only examined NSCs once encapsulated but not after recovery from the hydrogels.<sup>38</sup> Another study recovered viable NSCs that were encapsulated in calcium alginate beads; however, no changes in proliferation or differentiation were assessed.<sup>64</sup> Our group attempted immunocytochemistry experiments on cells encapsulated within hydrogels, however, because of the high background autofluorescence of the hydrogels, it was difficult to conduct quantitative analyses. Furthermore, adult neural stem cells are known to proliferate and differentiate into oligodendrocytes, astrocytes, and neurons *in vitro* when the growth factor is withdrawn. Because these specific cells do not need to be induced to differentiate via chemicals, we were interested to study the spontaneous differentiation of adult stem cells *in vitro*. Therefore, we provide a quantitative analysis of recovered AHPCs from alginate hydrogels in order to better understand how the 3D environment influenced cell proliferation and differentiation *in vitro*.

In addition to the previous literature, our interest focused on fabricating fibrous scaffolds for cell encapsulation using a microfluidic technique. Few studies have investigated cell encapsulation within alginate-based fibrous hydrogels fabricated using a microfluidic approach.<sup>65,66</sup> However, there has

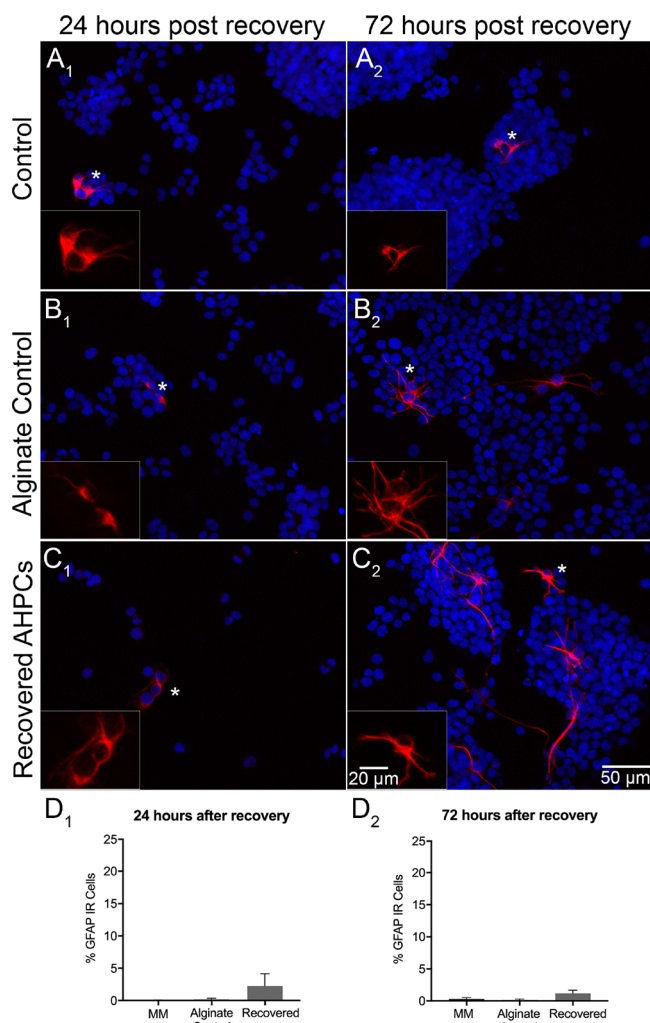


**Figure 4.** Glial differentiation of recovered AHPCs after 4 days of encapsulation. Fluorescence images of AHPCs illustrating immunoreactivity for GFAP 24 h after recovery (A<sub>1</sub>–C<sub>1</sub>) and 72 h after recovery (A<sub>2</sub>–C<sub>2</sub>): GFAP-Cy3 (red) with DAPI staining (blue). AHPCs cultured in MM (A<sub>1</sub>,A<sub>2</sub>), alginate control (B<sub>1</sub>,B<sub>2</sub>), and recovered from hydrogels (C<sub>1</sub>,C<sub>2</sub>). Asterisks indicate the location of the higher magnification inset images. Higher magnification images are of the GFAP-Cy3 channel only. Scale bar = 50  $\mu$ m (20  $\mu$ m for insets). Abbreviations: DAPI, 4',6-diamidino-2-phenylindole. (D<sub>1</sub>,D<sub>2</sub>), Quantitative analysis of AHPCs immunoreactive for the GFAP antibody. Error bars represent the standard error of the mean.  $N = 6$  independent experiments, 5 imaging fields per experiment.

cells from all conditions (control cells in MM, alginate control, and recovered AHPCs) was positive for GFAP immunolabeling, indicating glial differentiation is supported, no statistically significant differences between conditions were detected [ $(p \leq 0.05)$  (Figure 4D<sub>1</sub>,D<sub>2</sub>)]. These results support previous studies in which AHPCs in MM have less than 2% of cells differentiating into GFAP immunopositive cells, even after 6 DIV.<sup>50</sup>

been no report of encapsulation and recovery of AHPCs from alginate fibrous hydrogels. The microfluidic platform can be versatile when fabricating fibers, which can be used to better mimic the microenvironment of the native tissue. Fibers can be clinically relevant for guiding axon regrowth and guidance for spinal cord and peripheral nerve injuries,<sup>67</sup> as well as scaffolds to guide cell differentiation.<sup>35</sup> As used in our study, hydrogels are fibrous networks in which cells can grow and differentiate within, thus guiding cell differentiation.

One of the key influencers of cell migration and cell fate determination is the microenvironment created by the ECM.<sup>68,69</sup> The ECM is a complex network of fibrous proteins (such as fibronectin, laminin, and collagen) and carbohydrates that is crucial for providing mechanical cues that aid in cell adhesion and signaling *in vivo*, making it difficult to mimic *in vitro*.<sup>2</sup> Traditional 2D models face challenges in mimicking the native tissue present in the brain because of the lack of complex cell to ECM interactions. However, biomaterials such as hydrogels can serve as a platform to mimic the ECM present *in vivo*. Integrins on the cells' surface sense the mechanical properties within the ECM<sup>70</sup> and are important in cell adhesion and differentiation of NSCs. Integrin receptors are highly expressed in mammalian NSCs and involved in adhesion along with cell fate determination.<sup>71</sup> Integrins expressed in AHPCs play a crucial role in morphological differentiation.<sup>72</sup> Our results demonstrate that AHPCs that were encapsulated, recovered, and immunostained had increased proliferation and neuronal differentiation, indicating there may be a connection to signaling pathways utilizing integrin-mediated focal adhesions in this study. Particularly, cells encapsulated were within an environment in which cell–cell interactions may have been greater, thus leading to more proliferation at 24 h post recovery than 72 h, as demonstrated in our study. Although our 2D control did not entail AHPCs cultured on alginate surfaces, we were able to show that alginate does not influence the differentiation of cells using our control conditions. For our control conditions, AHPCs not encapsulated were exposed to alginate within culture as well as a control population of cells that were not exposed to encapsulation or alginate. We believe this is a sufficient control as we are hypothesizing that a 3D environment influences the differentiation of neural stem cells *in vitro*. Future studies may investigate the effect of encapsulating AHPCs within various alginate percentages and performing gene expression analyses that can help guide differentiation toward specific lineages.

Taken together, multiple studies have utilized materials, topographies, and mechanical properties to investigate ways to control cell proliferation and differentiation as well as gain a better understanding of how cells rely on the microenvironment for fate determination.<sup>73–75</sup> Our study focuses on the fate of cells post recovery as this is important in therapeutic strategies. Cell delivery *via* hydrogels is a promising approach for regenerative medicine and therefore must be studied in depth. Moreover, the ability to control stem cell proliferation and differentiation without chemical inducers is clinically relevant in neural tissue engineering.

## CONCLUSIONS

A microfluidic platform was used to encapsulate AHPCs within an alginate-based hydrogel. Our results show that hydrogels promote cell proliferation *in vitro* and support neuronal and glial differentiation. Hydrogels can be used to develop rationale strategies for cell transplantation because of their ability to

mimic the native microenvironment and direct cell differentiation. Hydrogels in combination with cell encapsulation and transplantation approaches can be used for multiple biomedical engineering applications including cellular therapies and drug- and gene-delivery strategies.

## AUTHOR INFORMATION

### Corresponding Author

Donald S. Sakaguchi – Department of Genetics, Development and Cell Biology, Neuroscience Program, and Biology Program, Iowa State University, Ames, Iowa 50011, United States;  
orcid.org/0000-0003-4537-0972; Phone: 515-294-3112;  
Email: dssakagu@iastate.edu; Fax: 515-294-8457

### Authors

Bhavika B. Patel – Department of Genetics, Development and Cell Biology and Neuroscience Program, Iowa State University, Ames, Iowa 50011, United States

Marilyn C. McNamara – Department of Mechanical Engineering, Iowa State University, Ames, Iowa 50011, United States

Laura S. Pesquera-Colom – Department of Genetics, Development and Cell Biology and Biology Program, Iowa State University, Ames, Iowa 50011, United States

Emily M. Kozik – Department of Genetics, Development and Cell Biology and Biology Program, Iowa State University, Ames, Iowa 50011, United States

Jasmin Okuzonu – Department of Biological and Chemical Engineering, Iowa State University, Ames, Iowa 50010, United States

Nicole N. Hashemi – Department of Mechanical Engineering, Iowa State University, Ames, Iowa 50011, United States;  
orcid.org/0000-0001-8921-7588

Complete contact information is available at:  
<https://pubs.acs.org/10.1021/acsomega.9b04214>

### Author Contributions

The manuscript was written through contributions of all authors. All authors have given approval to the final version of the manuscript.

### Funding

This work was partially supported by the Stem Cell Research Fund, the Department of Genetics, Development and Cell Biology, the Iowa State University College of Liberal Arts and Sciences Dean's High Impact Award for Undergraduate Research, the Office of Naval Research (ONR) grant N000141612246, and ONR grant N000141712620.

### Notes

The authors declare no competing financial interest.

## ACKNOWLEDGMENTS

The authors would like to thank Dr. F. Gage at the Salk Institute for the gift of the AHPCs.

## REFERENCES

- (1) Temple, S. The development of neural stem cells. *Nature* **2001**, *414*, 112–117.
- (2) Tibbitt, M. W.; Anseth, K. S. Hydrogels as extracellular matrix mimics for 3D cell culture. *Biotechnol. Bioeng.* **2009**, *103*, 655–663.
- (3) Nicodemus, G. D.; Bryant, S. J. Cell encapsulation in biodegradable hydrogels for tissue engineering applications. *Tissue Eng., Part B* **2008**, *14*, 149–165.

- (4) El-Sherbiny, I. M.; Yacoub, M. H. Hydrogel scaffolds for tissue engineering: Progress and challenges. *Global Cardiol. Sci. Pract.* **2013**, *2013*, 38.
- (5) Chan, B. P.; Leong, K. W. Scaffolding in tissue engineering: general approaches and tissue-specific considerations. *Eur. Spine J.* **2008**, *17*, 467–479.
- (6) Singh, A.; Peppas, N. A. Hydrogels and scaffolds for immunomodulation. *Adv. Mater.* **2014**, *26*, 6530–6541.
- (7) Lee, K. Y.; Mooney, D. J. Alginate: properties and biomedical applications. *Prog. Polym. Sci.* **2012**, *37*, 106–126.
- (8) Guarino, V.; Caputo, T.; Altobelli, R.; Ambrosio, L. Degradation properties and metabolic activity of alginate and chitosan poly-electrolytes for drug delivery and tissue engineering applications. *AIMS Mater. Sci.* **2015**, *2*, 497–502.
- (9) Sun, J.; Tan, H. Alginate-Based Biomaterials for Regenerative Medicine Applications. *Materials* **2013**, *6*, 1285–1309.
- (10) Sun, J.; Tan, H. Alginate-Based Biomaterials for Regenerative Medicine Applications. *Materials* **2013**, *6*, 1285–1309.
- (11) McNamara, M. C.; Sharifi, F.; Wrede, A. H.; Kimlinger, D. F.; Thomas, D.-G.; Vander Wiel, J. B.; Chen, Y.; Montazami, R.; Hashemi, N. N. Microfibers as Physiologically Relevant Platforms for Creation of 3D Cell Cultures. *Macromol. Biosci.* **2017**, *17*, 1700279.
- (12) McNamara, M. C.; Sharifi, F.; Okuzono, J.; Montazami, R.; Hashemi, N. N. Microfluidic Manufacturing of Alginate Fibers with Encapsulated Astrocyte Cells. *ACS Appl. Bio Mater.* **2019**, *2*, 1603–1613.
- (13) Stevens, M.; Qanadilo, H. F.; Langer, R.; Prasad Shastri, V. A rapid-curing alginate gel system: utility in periosteum-derived cartilage tissue engineering. *Biomaterials* **2004**, *25*, 887–894.
- (14) Venkatesan, J.; Bhatnagar, I.; Manivasagan, P.; Kang, K.-H.; Kim, S.-K. Alginate composites for bone tissue engineering: A review. *Int. J. Biol. Macromol.* **2015**, *72*, 269–281.
- (15) Bozza, A.; Coates, E. E.; Incitti, T.; Ferlin, K. M.; Messina, A.; Menna, E.; Bozzi, Y.; Fisher, J. P.; Casarosa, S. Neural differentiation of pluripotent cells in 3D alginate-based cultures. *Biomaterials* **2014**, *35*, 4636–4645.
- (16) Frampton, J. P.; Hynd, M. R.; Shuler, M. L.; Shain, W. Fabrication and optimization of alginate hydrogel constructs for use in 3D neural cell culture. *Biomed. Mater.* **2011**, *6*, 015002.
- (17) Tønnesen, H. H.; Karlsen, J. Alginate in drug delivery systems. *Drug Dev. Ind. Pharm.* **2002**, *28*, 621–630.
- (18) Ausili, E.; Paolucci, V.; Triarico, S.; Maestrini, C.; Murolo, D.; Focarelli, B.; Rendeli, C. Treatment of pressure sores in spina bifida patients with calcium alginate and foam dressings. *Eur. Rev. Med. Pharmacol. Sci.* **2013**, *17*, 1642–1647.
- (19) Jun, Y.; Kang, E.; Chae, S.; Lee, S.-H. Microfluidic spinning of micro- and nano-scale fibers for tissue engineering. *Lab Chip* **2014**, *14*, 2145–2160.
- (20) Sharifi, F.; Kurteshi, D.; Hashemi, N. Designing highly structured polycaprolactone fibers using microfluidics. *J. Mech. Behav. Biomed. Mater.* **2016**, *61*, 530–540.
- (21) Lee, B. R.; Lee, K. H.; Kang, E.; Kim, D.-S.; Lee, S.-H. Microfluidic wet spinning of chitosan-alginate microfibers and encapsulation of HepG2 cells in fibers. *Biomicrofluidics* **2011**, *5*, 022208.
- (22) Cheng, J.; Jun, Y.; Qin, J.; Lee, S.-H. Electrospinning versus microfluidic spinning of functional fibers for biomedical applications. *Biomaterials* **2017**, *114*, 121–143.
- (23) Man, Y.; Wang, P.; Guo, Y.; Xiang, L.; Yang, Y.; Qu, Y.; Gong, P.; Deng, L. Angiogenic and osteogenic potential of platelet-rich plasma and adipose-derived stem cell laden alginate microspheres. *Biomaterials* **2012**, *33*, 8802–8811.
- (24) Workman, V. L.; Dunnett, S. B.; Kille, P.; Palmer, D. D. Microfluidic chip-based synthesis of alginate microspheres for encapsulation of immortalized human cells. *Biomicrofluidics* **2007**, *1*, 014105.
- (25) Martinez, C. J.; Kim, J. W.; Ye, C.; Ortiz, I.; Rowat, A. C.; Marquez, M.; Weitz, D. A Microfluidic Approach to Encapsulate Living Cells in Uniform Alginate Hydrogel Microparticles. *Macromol. Biosci.* **2012**, *12*, 946–951.
- (26) Jiang, W.; Li, M.; Chen, Z.; Leong, K. W. Cell-laden microfluidic microgels for tissue regeneration. *Lab-on-a-Chip* **2016**, *16*, 4482–4506.
- (27) Martino, C.; Statzer, C.; Vigolo, D.; deMello, A. J. Controllable generation and encapsulation of alginate fibers using droplet-based microfluidics. *Lab Chip* **2016**, *16*, 59–64.
- (28) Sharifi, F.; Sooriyachchi, A. C.; Altural, H.; Montazami, R.; Rylander, M. N.; Hashemi, N. Fiber Based Approaches as Medicine Delivery Systems. *ACS Biomater. Sci. Eng.* **2016**, *2*, 1411–1431.
- (29) Kang, E.; Choi, Y. Y.; Chae, S.-K.; Moon, J.-H.; Chang, J.-Y.; Lee, S.-H. Microfluidic spinning of flat alginate fibers with grooves for cell-aligning scaffolds. *Adv. Mater.* **2012**, *24*, 4271–4277.
- (30) Gnani, S.; Fornasari, B. E.; Tonda-Turo, C.; Laurano, R.; Zanetti, M.; Ciardelli, G.; Geuna, S. The Effect of Electrospun Gelatin Fibers Alignment on Schwann Cell and Axon Behavior and Organization in the Perspective of Artificial Nerve Design. *Int. J. Mol. Sci.* **2015**, *16*, 12925–12942.
- (31) Gaharwar, A. K.; Nikkhah, M.; Sant, S.; Khademhosseini, A. Anisotropic poly (glycerol sebacate)-poly (-caprolactone) electrospun fibers promote endothelial cell guidance. *Biofabrication* **2014**, *7*, 015001.
- (32) Han, J.; Wu, Q.; Xia, Y.; Wagner, M. B.; Xu, C. Cell alignment induced by anisotropic electrospun fibrous scaffolds alone has limited effect on cardiomyocyte maturation. *Stem Cell Res.* **2016**, *16*, 740–750.
- (33) Wade, R. J.; Burdick, J. A. Engineering ECM signals into biomaterials. *Mater. Today* **2012**, *15*, 454–459.
- (34) Patel, B. B.; Sharifi, F.; Stroud, D. P.; Montazami, R.; Hashemi, N. N.; Sakaguchi, D. S. 3D Microfibrous Scaffolds Selectively Promotes Proliferation and Glial Differentiation of Adult Neural Stem Cells: A Platform to Tune Cellular Behavior in Neural Tissue Engineering. *Macromol. Biosci.* **2019**, *19*, 1800236.
- (35) Sharifi, F.; Patel, B. B.; Dzuilko, A. K.; Montazami, R.; Sakaguchi, D. S.; Hashemi, N. Polycaprolactone Microfibrous Scaffolds to Navigate Neural Stem Cells. *Biomacromolecules* **2016**, *17*, 3287–3297.
- (36) Lewicki, J.; Bergman, J.; Kerins, C.; Hermanson, O. Optimization of 3D bioprinting of human neuroblastoma cells using sodium alginate hydrogel. *Bioprinting* **2019**, *16*, No. e00053.
- (37) Ashton, R. S.; Banerjee, A.; Punyani, S.; Schaffer, D. V.; Kane, R. S. Scaffolds based on degradable alginate hydrogels and poly(lactide-co-glycolide) microspheres for stem cell culture. *Biomaterials* **2007**, *28*, 5518–5525.
- (38) Banerjee, A.; Arha, M.; Choudhary, S.; Ashton, R. S.; Bhatia, S. R.; Schaffer, D. V.; Kane, R. S. The influence of hydrogel modulus on the proliferation and differentiation of encapsulated neural stem cells. *Biomaterials* **2009**, *30*, 4695–4699.
- (39) Li, X.; Liu, T.; Song, K.; Yao, L.; Ge, D.; Bao, C.; Ma, X.; Cui, Z. Culture of neural stem cells in calcium alginate beads. *Biotechnol. Prog.* **2006**, *22*, 1683–1689.
- (40) Moxon, S. R.; Corbett, N. J.; Fisher, K.; Potjewyd, G.; Domingos, M.; Hooper, N. M. Blended alginate/collagen hydrogels promote neurogenesis and neuronal maturation. *Mater. Sci. Eng., C* **2019**, *104*, 109904.
- (41) Ho, S. S.; Murphy, K. C.; Binder, B. Y. K.; Vissers, C. B.; Leach, J. K. Increased Survival and Function of Mesenchymal Stem Cell Spheroids Entrapped in Instructive Alginate Hydrogels. *Stem Cells Transl. Med.* **2016**, *5*, 773–781.
- (42) Ansari, S.; Chen, C.; Xu, X.; Annabi, N.; Zadeh, H. H.; Wu, B. M.; Khademhosseini, A.; Shi, S.; Moshaverinia, A. Muscle Tissue Engineering Using Gingival Mesenchymal Stem Cells Encapsulated in Alginate Hydrogels Containing Multiple Growth Factors. *Ann. Biomed. Eng.* **2016**, *44*, 1908–1920.
- (43) Hunt, N. C.; Hallam, D.; Karimi, A.; Mellough, C. B.; Chen, J.; Steel, D. H. W.; Lako, M. 3D culture of human pluripotent stem cells in RGD-alginate hydrogel improves retinal tissue development. *Acta Biomater.* **2017**, *49*, 329–343.



- (44) Wilson, J. L.; Najia, M. A.; Saeed, R.; McDevitt, T. C. Alginate encapsulation parameters influence the differentiation of micro-encapsulated embryonic stem cell aggregates. *Biotechnol. Bioeng.* **2014**, *111*, 618–631.
- (45) Cao, H.; Liu, T.; Chew, S. Y. The application of nanofibrous scaffolds in neural tissue engineering. *Adv. Drug Delivery Rev.* **2009**, *61*, 1055–1064.
- (46) Liang, D.; Hsiao, B. S.; Chu, B. Functional electrospun nanofibrous scaffolds for biomedical applications. *Adv. Drug Delivery Rev.* **2007**, *59*, 1392–1412.
- (47) Bai, Z.; Mendoza Reyes, J. M.; Montazami, R.; Hashemi, N. On-chip development of hydrogel microfibers from round to square/ribbon shape. *J. Mater. Chem. A* **2014**, *2*, 4878–4884.
- (48) Hashemi, N.; Erickson, J. S.; Golden, J. P.; Ligler, F. S. Optofluidic characterization of marine algae using a microflow cytometer. *Biomicrofluidics* **2011**, *5*, 032009.
- (49) Gage, F. H.; Coates, P. W.; Palmer, T. D.; Kuhn, H. G.; Fisher, L. J.; Suhonen, J. O.; Peterson, D. A.; Suhr, S. T.; Ray, J. Survival and differentiation of adult neuronal progenitor cells transplanted to the adult brain. *Proc. Natl. Acad. Sci. U.S.A.* **1995**, *92*, 11879–11883.
- (50) Oh, J.; Daniels, G. J.; Chiou, L. S.; Ye, E.-A.; Jeong, Y.-S.; Sakaguchi, D. S. Multipotent adult hippocampal progenitor cells maintained as neurospheres favor differentiation toward glial lineages. *Biotechnol. J.* **2014**, *9*, 921–933.
- (51) Schindelin, J.; Arganda-Carreras, I.; Frise, E.; Kaynig, V.; Longair, M.; Pietzsch, T.; Preibisch, S.; Rueden, C.; Saalfeld, S.; Schmid, B.; Tinevez, J.-Y.; White, D. J.; Hartenstein, V.; Eliceiri, K.; Tomancak, P.; Cardona, A. Fiji: an open-source platform for biological-image analysis. *Nat. Methods* **2012**, *9*, 676.
- (52) Sharifi, F.; Bai, Z.; Montazami, R.; Hashemi, N. Mechanical and physical properties of poly(vinyl alcohol) microfibers fabricated by a microfluidic approach. *RSC Adv.* **2016**, *6*, 55343–55353.
- (53) Scholzen, T.; Gerdes, J. The Ki-67 protein: from the known and the unknown. *J. Cell. Physiol.* **2000**, *182*, 311–322.
- (54) Seidlits, S. K.; Khaing, Z. Z.; Petersen, R. R.; Nickels, J. D.; Vanscoy, J. E.; Shear, J. B.; Schmidt, C. E. The effects of hyaluronic acid hydrogels with tunable mechanical properties on neural progenitor cell differentiation. *Biomaterials* **2010**, *31*, 3930–3940.
- (55) Gage, F. H. Mammalian neural stem cells. *Science* **2000**, *287*, 1433–1438.
- (56) Joshi, H. C.; Cleveland, D. W. Differential utilization of beta-tubulin isoforms in differentiating neurites. *J. Cell Biol.* **1989**, *109*, 663.
- (57) Lee, M. K.; Rebhun, L. I.; Frankfurter, A. Posttranslational modification of class III beta-tubulin. *Proc. Natl. Acad. Sci. U.S.A.* **1990**, *87*, 7195–7199.
- (58) Daniele, M. A.; Boyd, D. A.; Adams, A. A.; Ligler, F. S. Microfluidic strategies for design and assembly of microfibers and nanofibers with tissue engineering and regenerative medicine applications. *Adv. Healthcare Mater.* **2015**, *4*, 11–28.
- (59) Chen, J. S.; Guan, C.; Gui, Y.; Blackwood, D. J. Rational Design of Self-Supported Ni<sub>3</sub>S<sub>2</sub> Nanosheets Array for Advanced Asymmetric Supercapacitor with a Superior Energy Density. *ACS Appl. Mater. Interfaces* **2017**, *9*, 496–504.
- (60) Sun, T.; Li, X.; Shi, Q.; Wang, H.; Huang, Q.; Fukuda, T. Microfluidic Spun Alginate Hydrogel Microfibers and Their Application in Tissue Engineering. *Gels* **2018**, *4*, 38.
- (61) Zhang, X.; Weng, L.; Liu, Q.; Li, D.; Deng, B. Facile fabrication and characterization on alginate microfibres with grooved structure via microfluidic spinning. *R. Soc. Open Sci.* **2019**, *6*, 181928.
- (62) Hosseini, S. M.; Sharafkhan, A.; Koohi-Hosseinabadi, O.; Semsar-Kazerooni, M. Transplantation of Neural Stem Cells Cultured in Alginate Scaffold for Spinal Cord Injury in Rats. *Asian Spine J.* **2016**, *10*, 611–618.
- (63) Ashton, R. S.; Banerjee, A.; Punyani, S.; Schaffer, D. V.; Kane, R. S. Scaffolds based on degradable alginate hydrogels and poly(lactide-co-glycolide) microspheres for stem cell culture. *Biomaterials* **2007**, *28*, 5518–5525.
- (64) Li, X.; Liu, T.; Song, K.; Yao, L.; Ge, D.; Bao, C.; Ma, X.; Cui, Z. Culture of Neural Stem Cells in Calcium Alginate Beads. *Biotechnol. Prog.* **2006**, *22*, 1683–1689.
- (65) Hidalgo San Jose, L.; Stephens, P.; Song, B.; Barrow, D. Microfluidic Encapsulation Supports Stem Cell Viability, Proliferation, and Neuronal Differentiation. *Tissue Eng., Part C* **2018**, *24*, 158–170.
- (66) Ling, Y.; Rubin, J.; Deng, Y.; Huang, C.; Demirci, U.; Karp, J. M.; Khademhosseini, A. A cell-laden microfluidic hydrogel. *Lab Chip* **2007**, *7*, 756–762.
- (67) Rossi, S.; Vigani, B.; Sandri, G.; Bonferoni, M. C.; Ferrari, F. Design and criteria of electrospun fibrous scaffolds for the treatment of spinal cord injury. *Neural Regen. Res.* **2017**, *12*, 1786–1790.
- (68) Burdick, J. A.; Vunjak-Novakovic, G. Engineered Microenvironments for Controlled Stem Cell Differentiation. *Tissue Eng., Part A* **2009**, *15*, 205–219.
- (69) Engler, A. J.; Sen, S.; Sweeney, H. L.; Discher, D. E. Matrix Elasticity Directs Stem Cell Lineage Specification. *Cell* **2006**, *126*, 677–689.
- (70) Howe, A.; Aplin, A. E.; Alahari, S. K.; Juliano, R. Integrin signaling and cell growth control. *Curr. Opin. Cell Biol.* **1998**, *10*, 220–231.
- (71) Campos, L. S.; Decker, L.; Taylor, V.; Skarnes, W. Notch, epidermal growth factor receptor, and beta1-integrin pathways are coordinated in neural stem cells. *J. Biol. Chem.* **2006**, *281*, 5300–5309.
- (72) Harper, M. M.; Ye, E.-A.; Blong, C. C.; Jacobson, M. L.; Sakaguchi, D. S. Integrins Contribute to Initial Morphological Development and Process Outgrowth in Rat Adult Hippocampal Progenitor Cells. *J. Mol. Neurosci.* **2010**, *40*, 269–283.
- (73) Lavik, E. B.; Klassen, H.; Warfvinge, K.; Langer, R.; Young, M. J. Fabrication of degradable polymer scaffolds to direct the integration and differentiation of retinal progenitors. *Biomaterials* **2005**, *26*, 3187–3196.
- (74) Guvendiren, M.; Burdick, J. A. The control of stem cell morphology and differentiation by hydrogel surface wrinkles. *Biomaterials* **2010**, *31*, 6511–6518.
- (75) Lim, S. H.; Liu, X. Y.; Song, H.; Yarema, K. J.; Mao, H.-Q. The effect of nanofiber-guided cell alignment on the preferential differentiation of neural stem cells. *Biomaterials* **2010**, *31*, 9031–9039.